



Photodynamic Therapy and Lung Cancer Stem Cells – The effects of AIPcS₄Cl on Isolated Lung Cancer Stem Cells

Anine Crous^a, Heidi Abrahamse^{b1}

^{a,b} *Laser Research Centre, Faculty of Health Sciences, University of Johannesburg, PO Box 17011, Johannesburg 2028, South Africa*

Abstract

Cancer is a worldwide burden. Claiming the lives of millions annually. Lung cancer is the leading contributor to mortality rates caused by cancer. Lowering risk factors such as tobacco consumption and industrial pollution can reduce lung cancer incidence. Yet it is noted to be counter-intuitive in emerging nations. An important disease entity is people who develop lung cancer regardless of avoiding factors leading to cancer. A subset of cells known to contribute to the high mortality rates seen in lung cancer is cancer stem cells (CSCs). Studies on CSCs have shown that they can evade conventional cancer treatment. Attributing to their stem-like characteristics is self-renewal, differentiation leading to phenotypical heterogeneity of tumor cells, metastasis and cancer recurrence. Expression of genetic markers involved in drug efflux, regeneration and motility contribute to the stem-like nature of CSCs. Photodynamic therapy (PDT) is an effective yet underutilized treatment modality for a variety of cancers. This form of alternative chemotherapy uses a non-toxic drug that has an affinity for cancerous cells. The drug localizes in intracellular organelles exerting an effect upon laser activation of the drug at a specific wavelength. Extensive research has been focused on the development of operative photosensitizers (PS), enhancing its selectivity and uptake into cancerous cells. Aluminium (III) Phthalocyanine Chloride Tetrasulphonate (AIPcS₄Cl) is an improved second generation PS with ideal PDT characteristics including high photochemical reactivity, it is amphiphilic, has low dark toxicity, good localization and little light sensitivity. The effects and efficacy of PSs in the eradication of CSCs are not well studied. PDT can be a useful therapeutic tool in the eradication of CSCs, where factors such as fluence, dose, and localization play a crucial role. In this study, we evaluated the effects of (AIPcS₄Cl) on isolated lung CSCs expressing stem-like markers involved in metastasis and drug resistance. Our findings suggest that treating CSCs using PDT is advantageous over standard cancer treatments. The results can be attributed to PDT not inducing drug resistance upon initial application of treatment to CSCs. This is due to passive absorption of the PDT drug which doesn't activate drug efflux pumps in the CSCs. This enables the PS to localize in the cell, ensuring biochemical responses upon laser activation leading to cellular toxicity and cellular death.

Keywords:

Photodynamic Therapy,
Photosensitizer,
Lung Cancer Stem Cells,
Surface Markers,
Cell Death,
Cytotoxicity,
Proliferation,
Viability.

1. Introduction

Malignancy is a disease that had formed part of a global problem over many decades. It has driven broad research and modern medicine to seek prevention and treatment to combat cancer and its mortality rates. Along with preventative treatment research, the causes of cancer and its dynamics are also investigated [1]. Cancer development starts on a cellular level where genetic mutations lead to defective instructions in the DNA sequence. These mutations can affect normal cell cycle function where the cells evade apoptosis along with genetic instability contributing to further cancer-promoting mutations [2]. Along with cancer cells evading cell cycle arrest cancer can have the ability to metastasize and return even after conventional therapy.

Lung cancer is a noteworthy supporter of disease fatalities. Carcinoma of the lung emerges because of hazardous factors, for example, smoking, inhalation of destructive synthetics and air contamination; prompting mutagenic transformations of typical lung tissue. Along with risk factors promoting lung cancer development there are still patients who avoid these risks, yet are still the victim of mutagens leading to cancer development. These genetic transformations

¹ CONTACT: habrahamse@uj.ac.za

cause hereditary adjustments that can change cell cycle regulations, prompting cellular expansion, tissue invasion, tumor development and metastasis [3]. Patients undergoing lung cancer treatment can still only expect a 5-year survival rate. This is due to treatment resistance before and during chemo and radiation therapy. Treatment resistance contributes to disease progression, recurrence and mortality [4]. This poses a significant clinical challenge for lung cancer treatment. Novel agents have been used alone and in combination with conventional therapy to overcome this problem. However, the basic systems presenting this resistant phenotype in malignant lung growth stay obscure [5]. The complete treatment of cancer depends on revealing its origin.

Research findings suggest that a small heterogeneous subpopulation of cells are the origin for cancer development. This small population of cells display stem-like characteristics. These cells are called cancer stem cells (CSCs). CSCs can self-renew, have multi-differentiation potential and are known to evade drug-induced cell death and can metastasize [6]. CSCs differ from the bulk of a tumor by its characteristic ability to repopulate a malignant growth. Giving rise to both CSCs and non-stem cancerous cells. Asymmetric division enables the CSCs to self-perpetuate and generate a differentiated progeny. Giving rise to a heterogeneous tumor whilst maintaining the CSC subpopulation. CSCs undergo symmetric division during periods of stress. Whereas non-stem-like lung cancer cells undergo only symmetric division. Resulting in a pure non-CSC cell population. This may explain the ineffectiveness of many conventional therapies and patient relapse [5]. These important clinical observations have stimulated intense interest in experimental approaches for further investigation of CSCs and their role in the treatment of drug resistant lung cancer. CSCs show strong treatment opposition and endurance because of expanded telomere length, initiation against apoptotic pathways, expanded membrane transporter action and their capacity to relocate and metastasize [7]. Lung CSCs identified, showed resistance to various lung cancer treatment options. These include: conventional therapy, biological molecules and targeted therapy. Eliminating lung CSCs during therapeutic intervention is of utmost importance. As this can prevent CSC expansion, cancer recurrence, relapse and metastasis. While little is at present known about lung CSC biology, various CSC markers have been distinguished and considered. These markers incorporate ALDH1, CD133, side population (Hoechst-negative), CD44, CD87 and CD117. These markers have been connected to chemo resistance in various first line disease treatments [5]. It is therefore widely accepted that CSCs are closely related to pathological features resulting in poor clinical prognosis [8].

Photodynamic therapy (PDT) or Alternate/ Photo chemotherapy is an innovative form of cancer treatment. PDT is not intrusive and can be used as a stand-alone treatment or in combination with conventional cancer treatments showing excellent therapeutic outcomes [9]. Non-oncological diseases can also benefit from PDT. It has been successfully used in dermatology, oncology, gynecology and urology. The photosensitive compound or photosensitizer (PS) is used either locally or applied systemically. Where it concentrates in malignant tissues. This leads to selective destruction of cancerous cells via the absorption of light from a particular wavelength. Due to its selectivity, this form of treatment is well tolerated by patients. Despite PDT achieving high success rates in treating various cancers. Researchers are investigating the improvement of PDT by enhancing its selectivity and effectiveness by developing new PS compounds and improving PS delivery methods [10].

The mechanism of action for PDT comprises of the photosensitive compound being activated through photon absorption from a specific light wave. The activated PS generates reactive oxygen species (ROS) leading to cell membrane damage and cell death. The PS moves from its ground state to its excited singlet state. The PS in its excited triplet state can follow two pathways. Type I the PS reacts with biomolecules, transferring hydrogen atoms via the radical mechanism generating free radicals and radical ions. These radicals then react with oxygen resulting in ROS generation. Type II the PS reacts with oxygen in its triplet ground state. Yielding singlet oxygen which is highly reactive and cytotoxic [11].

Characteristics of an ideal PS include no dark toxicity, little aggregation, photo stability, absorbs light at long wavelengths, high singlet oxygen yield, fluorescent, minimum daylight absorption, is not retained by non-cancerous cells and is highly concentrated in cancerous tissue [12]. Clinical anticancer therapy uses the first generation PSs from the porphyrin class. However, these PS tend to have important drawbacks such as short wavelength light absorption that can interfere with tissue absorption. They have low extinction coefficients and induces photosensitivity of the skin [13]. Phthalocyanines (Pc) are synthetic dyes that have a high molar absorption coefficient in the red part of the spectrum. Pcs belong to the group of 2nd generation PSs which exhibit a high extinction coefficient around 670 and 750 nm and even up to 1,000 nm. Thus allowing increased tissue penetration of the activating light [14]. Most phthalocyanine derivatives exhibit high hydrophobicity, which limits their clinical efficacy [13]. Modifying the axial and peripheral substituents changes the tendency for aggregation, pharmacokinetics, bio distribution, solubility, as well as fine-tuning of near infrared (NIR) absorbance. Extinction coefficients higher than $10^5 \text{ M}^{-1} \text{ cm}^{-1}$ have been reported [15]. These mixes are porphyrin-like PSs, showing tetrapyrrolic, aromatic macrocycles with each cycle connected to the next by nitrogen particles. Each pyrrolic ring is reached out by a benzene ring bringing about the red-shift of their last retention band. Attaching substituents to the peripheral and non-peripheral ring sites can alter the Q band location and complexity of a Pc. Furthermore, the Pc can be adjusted depending on the substituents nature, size and number. Electron donating groups, for example, $-\text{NH}_2$, OR and SR at the non-peripheral and periphery result in a red shift to the NIR area. Substitution at

the non-peripheral position indicates more red-shift than at the peripheral position [16]. Other than their solid assimilation in the NIR, Pcs show low retention at wavelengths somewhere in the range of 400 and 600 nm driving possibly to a lower skin photosensitization when presented to daylight. In addition, the nearness of a diamagnetic focal metal, for example, Al³⁺ in the Pc core appears to improve the triplet state life time (τ), just as its yield (Φ_t) and singlet oxygen yields (Φ_Δ) contrasted with paramagnetic metals [15]. Low lethality of phthalocyanines makes them promising for PDT application. Both lipophilic and water-dissolvable phthalocyanines have been considered as a possibility for PDT. Sulfonation essentially expands Pc dissolvability in polar solvents including water, evading the requirement for elective conveyance vehicles [14]. When comparing sulfonated AIPc (AIPcS₄) to other PSs, such as porphyrin and a hydrophobic hydroxyphenylchlorin, most frequently used in clinical settings. AIPcS₄ showed increased cellular uptake [17], due to sulfonation enhancing its hydrophilic nature it is more acceptable to antibody conjugation. Even when compared to a hydrophilic form of porphyrin, AIPcS₄ has much better photochemical characteristics for use in PDT ($\epsilon_{675} = 1.7 \times 10^5$ vs. $\epsilon_{595} = 7 \times 10^3 \text{ M}^{-1}\text{cm}^{-1}$) [18]. Proving that Pc have a vast array of photo physical and spectral characteristics [15]. Aluminium (III) Phthalocyanine Chloride Tetrasulphonate (AIPcS₄Cl) is an improved second generation PS with ideal PDT characteristics. Along with the afore mentioned characteristics AIPcS₄Cl shows little to no dark toxicity and is amphiphilic in nature due to it being both water soluble and can bind to cytochrome c located in the mitochondrial membrane [14].

The CSC theory has attracted the development of targeted therapies. These therapies are aimed at destroying CSCs specifically, not only reducing the tumor bulk but cancer as a whole. PDT should not be viewed as a replacement therapy but rather as an adjunct to conventional cancer treatment. The concentration of PSs in cancerous cells alone could provide a solution for CSC resistance. PDT can, therefore, be used as an alternative treatment for lung cancer. Or combination treatment alongside standard cancer therapies in advanced cases. Current research is focused on finding a therapeutic modality that eradicates both the cancer tissue and the more resistant CSCs. The novel application of the eradication of CSCs using PDT will provide insight into the therapeutic potential of PDT in the treatment of lung cancers. Successful killing of CSCs in due course will reduce cases of treatment failures, recurrences and progression to other sites, subsequently driving down the disease burden of lung cancer in the world.

2. Materials and methods

To date, because so little is known regarding the response of CSCs to PDT, the aim of this research was to observe the cellular responses of lung CSCs after exposure to PDT using laser light and Aluminium (III) Phthalocyanine Chloride Tetrasulphonate (AIPcS₄Cl) (Frontier Scientific, AIPcS-834) as a PS. A side population of cells, isolated from the lung cancer cell line A549 (ATCC®, CCL185™), positive for the CSC antigenic markers CD 133, CD 56 and CD 44 were isolated using antibody conjugated magnetic microbeads and were verified by fluorescent protein detection using flow cytometry and immunofluorescent (IFL) microscopy. Localization of the PS was established in order to determine the effectiveness that PDT may have on CSCs using fluorescence (FL) and differential interference contrast (DIC) microscopy. The isolated lung CSCs received treatment using AIPcS₄Cl for PDT. Post irradiation biochemical responses were measured in order to establish the anticancer effect of AIPcS₄Cl on lung CSCs after 24h. These assays included morphology of cells, LDH cytotoxicity, ATP proliferation, Trypan Blue viability and Annexin VPI cell death. Reagent grade solvents and reagents were used as received.

2.1. Cell culture

Commercially accessible epithelial lung carcinoma cells from the ATCC were utilized in this investigation A549 (ATCC®, CCL185™). The media utilized for maintaining of the lung cancer cells and separated CSCs comprised of the accompanying: Rosewell Park Memorial Institute 1640 medium (RPMI-1640) (SIGMA, R8758) enhanced with 10% fetal bovine serum (FBS) (Biochrom, S0615) and 0.5% penicillin/streptomycin (SIGMA, P4333) and 0.5% amphotericin B (SIGMA, A2942).

Cell lines used for control purposes in the characterization of the isolated lung CSCs included: Colorectal adenocarcinoma cells Caco2 (Cellonex, Caco-2) were cultured in Dulbecco's Modified Eagle's Medium - high glucose, with 4500 mg/L glucose, L-glutamine, and sodium bi carbonate (DMEM) (SIGMA, D5796) supplemented with 10% FBS, 4 mM Sodium pyruvate solution (SIGMA, S8636), 0.5% penicillin/ streptomycin and 0.5% amphotericin B.

Uterine epithelial cells consistent with leiomyosarcoma SK-UT-1 (ATCC® HTB-114™) was cultured in Minimum Essential Medium Eagle, with Earle's salts and sodium bicarbonate (MEM) supplemented with 1% MEM Non-essential Amino Acid Solution (NEAA) (SIGMA, M7145), 2 mM L-glutamine (SIGMA, G7513), 1 mM sodium pyruvate, 10% FBS and 0.5% penicillin/ streptomycin and 0.5% amphotericin B.

Skin fibroblast cells WS1 (ATCC® CRL-1502™) were cultivated in MEM, supplemented with 1% NEAA, 2 mM L-glutamine, 1 mM sodium pyruvate, 10% FBS and 0.5% penicillin/ streptomycin and 0.5% amphotericin B.

Mesenchymal stem cells immortalized with hTERT ASC52telo (ATCC® SCRC-4000™) were cultured in Mesenchymal Stem Cell Basal Medium (ATCC® PCS-500-030™) supplemented with Mesenchymal Stem Cell Growth Kit (ATCC® PCS-500-040™).

All cultured cells were maintained and incubated at 37°C in 5% CO₂ and 85% humidity.

2.2. Isolation of CSCs

A magnetic bead isolation pack and division unit (Miltenyi Biotec, QuadroMACS™ partition unit 130-091-051) was utilized to separate lung CSCs from lung cancer cells. The cells were magnetically labelled with microbead conjugated antibodies coordinated at the antigenic surface marker CD 133, CD 56 and CD44. The cell populace was enhanced for CD 133+, CD 56+ and CD 44+ lung CSCs by utilizing the CD 133/CD 56/CD 44 MicroBead Kit (Miltenyi Biotec, MicroBead Kit, human 130-050-801) intended for the positive selection of cells expressing the human CD 133/CD 56 and CD 44 antigen. Cells were suspended and counted. The cell suspension was re-suspended in 80 µl buffer and 20 µl Micro-beads per 10⁷ total cells, followed by incubation for 15 minutes at 4°C. Cells were washed 3 times using buffer and centrifugation at 3000rpm for 10 min., and re-suspended in 500 µl buffer per 10⁷ cells. Cells homogeneously suspended in buffer were then added to prepared separation columns (Miltenyi Biotec, 130-042-201). Unlabeled cells are collected and discarded passing through the column, whereas positively selected cells that are conjugated to the magnetic beads would remain in the magnetic column, and flushed out into a suitable collection tube using buffer and a plunger.

2.3. Characterization of isolated lung CSCs

2.3.1. Flow Cytometry

To confirm whether cells isolated using the magnetic bead kit, were of CSC origin, cells were fluorescently labelled using the secondary antibody conjugation technique. Primary mouse anti human antibody CD133, CD 56 and CD44 was used. Isolated cells were placed in a suspension where they were washed twice using centrifugation and resuspension with ice-cold washing buffer: PBS/BSA/azide buffer (PBS/ 0.1% w/v bovine serum albumin (BSA) (Sigma, A2153)/ 0.01% w/v azide (Sigma, S8032)), and then incubated with blocking buffer (10 % (w/v) BSA (bovine serum albumin) 30 min on ice as a blocking step and washed twice as previously described. Cells were then incubated with primary mouse anti human antibody in working buffer (2% serum in PBS BSA/azide buffer) for 30 min, keeping the cells suspended in tubes on ice. Cells were then rinsed three times with washing buffer and incubated with secondary fluorescent (FL) antibodies FITC Goat anti-Mouse (NovusBio, NB720-F-1mg), Cy5 Goat anti-Mouse (NovusBio, NB7602) and PE Goat anti-Mouse (NovusBio, NB7594) in working buffer for 30 min on ice, protected from light where after they were washed again with washing buffer. The antigenic detection was done using the BD Accuri™ C6 flow cytometer (BD Biosciences, BD ACCURI C6) which detects the fluorescence on the conjugated antibody, indicating if the cells are CD 133, CD 56 and CD 44 positive/negative.

2.3.2. Immuno Fluorescence

The isolated CSCs were characterized using indirect immunofluorescence (IFL) a method that uses FL imaging detection. Whereby cultured cells are labelled with a primary antibody directed at a target antigen and made visible using fluorochromes attached to secondary antibodies directed at the primary antibodies.

Cells were cultured on heat-sterilized coverslips placed in petri dishes (3.5 cm culture dish, Corning, 430588), at a concentration of 5 x 10⁵ cells in complete media. Cells were incubated and allowed to attach to the coverslip. After cells were cultured on the coverslips, they were washed twice with ice-cold washing buffer: PBS/BSA/azide buffer (PBS/ 0.1% w/v bovine serum albumin (BSA) (Sigma, A2153)/ 0.01% w/v azide (Sigma, S8032)), and then incubated with blocking buffer (10 % (w/v) BSA (bovine serum albumin) for 30 min on ice as a blocking step and washed twice again using ice cold buffer.

Cells were then incubated with 100 µl primary mouse anti human antibody (CD133 Antibody; CD 56 Monoclonal Anti-N Cam; CD44 Antibody), in working buffer (2% serum in PBS BSA/azide buffer) for 30 min on ice. Cells were then rinsed three times with washing buffer. The cells were then labelled and incubated with 100 µl of the secondary FL FITC Goat anti-Mouse (NovusBio, NB720-F-1mg), Cy5 Goat anti-Mouse (NovusBio, NB7602) and PE Goat anti-Mouse (NovusBio, NB7594) antibody, in working buffer for 30 min on ice, protected from light. Cells were rinsed three times as before and fixed in 4 % Paraformaldehyde (Sigma, P6148) for 10 minutes. After fixation, cells were rinsed once briefly with PBS, before being stained with 4'- 6- diamidino-2-phenylindole (DAPI) (Invitrogen™, D1306) 358Ex/461Em and mounted on glass slides using Fluoromount™ Aqueous Mounting Medium (Sigma, F4680). Slides were viewed using a FL microscope, live cell station from Zeiss (Zeiss, Axio Observer Z1). The images were compiled using a Java image processing program ImageJ developed at the National Institutes of Health and the Laboratory for Optical and Computational Instrumentation, License: Public Domain, BSD-2.

2.4. Localization of AlPcS₄Cl in intracellular organelles of lung CSCs

Localization of AlPcS₄Cl into lung CSC cellular organelles was confirmed by FL and DIC microscopy, in order to establish the suitability of AlPcS₄Cl as a PS for PDT. Intracellular organelles such as mitochondria and lysosomes were fluorescently labelled. Cells were grown on glass coverslips in 35 mm culture dishes in complete media, at a seeding density of 5×10^5 cells until the cells have attached. Once the cells were attached, they received AlPcS₄Cl at a concentration of 20 μ M which was used as the treatment concentration. The cells were incubated for at least 4 hours allowing the PS to penetrate the cells. Cells were then washed with HBSS and stained with MitoTracker™ Green FM 490Ex/516EM (Invitrogen™, M7514) for mitochondria at a working concentration of 100 nM or LysoTracker™ Green DND-26 504Ex/511EM (Invitrogen™, L7526) for lysosomes using a working concentration of 50 nM for 30 min. Cells were then washed with HBSS and counterstained using DAPI. Cells were then rinsed with PBS, and excess buffer from the coverslip drained. Coverslips were then mounted onto glass microscope slides. Where after the slides were examined using the live cell station from Zeiss (Zeiss, Axio Observer Z1) to determine localization of the AlPcS₄Cl. Images were compiled using ImageJ.

2.5. Photodynamic Therapy

2.5.1. Photosensitizer

The PS Al (III) Phthalocyanine Chloride Tetrasulfonic Acid (AlPcS₄Cl) (Frontier Scientific, AlPcS-834) was used in this study. Its formula is C₃₂H₁₆AlClN₈O₁₂S₄, formula weight 895.21, TLC > 95 % with an absorbance wavelength of 674 nm. Figure 1 shows the structural components of AlPcS₄Cl. A predetermined concentration of the PS was used as established in a previous study conducted using AlPcS₄Cl on A549 lung cancer cells where a concentration of 20 μ M delivered an inhibitory concentration of 50 % [IC 50] along with a predetermined laser energy output of 10 J/cm² [19].

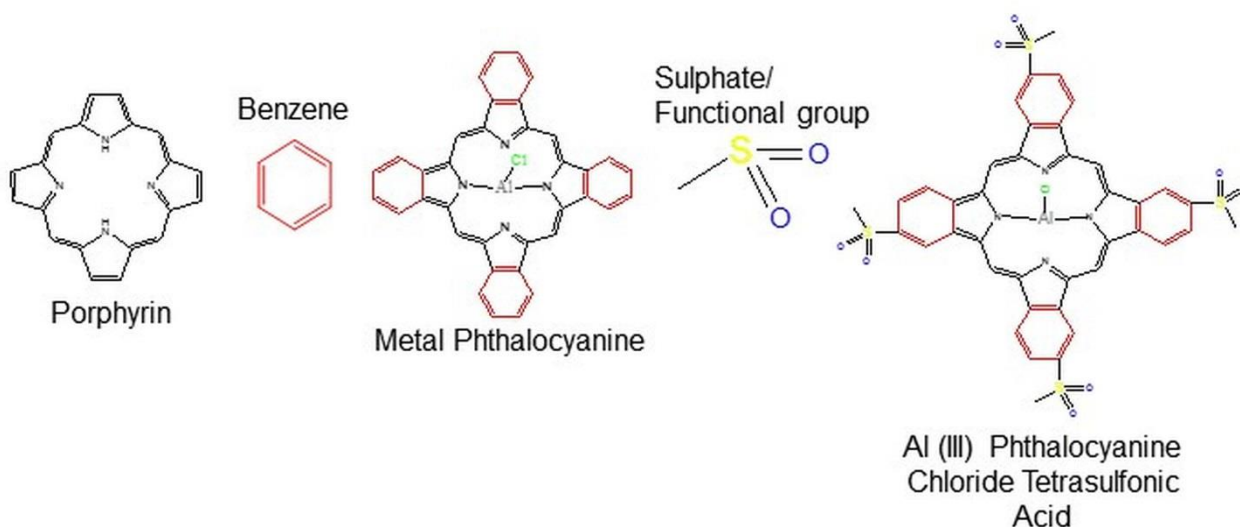


Figure 1. Structural components of AlPcS₄Cl, comprising of a porphyrin ring, pyrrolic/benzene rings and sulphate functional groups attached to a metalized phthalocyanine.

2.5.2. Laser irradiation

A 673.2 nm diode laser (Arroyo, High Power Laser, 1000 mA Laser source 4210 (S/N 070900108)) provided by the National Laser Center of South Africa, was used to irradiate the cells. Prior to exposing the cells to irradiation, the power output of the laser was measured using a FieldMate Laser Power Meter (FieldMate, Coherent, Power Sens detector (0496005)). The value from the meter reader was used to calculate the exposure time. Laser parameters are seen in Table 1.

Table 1. PDT drug and laser parameters using the 673.2 nm diode laser.**PARAMETERS**

Laser type	Semiconductor (Diode)
Wavelength (nm)	673.2
Wave emission	Continuous
Fluence (J/cm²)	10
Photosensitiser (PS)	AlPcS ₄ Cl
PS Concentration (μM)	20

The laser is setup with a fiber optic to deliver red light onto the monolayer of cells. The fiber optic is placed 8 cm above the cell culture dish, giving an irradiation spot size of 9.1 cm² covering the entire area of the culture dish. Cells were irradiated without the culture dish lid on at room temperature. In order to eliminate light interference, all irradiation protocols were performed in the dark. Irradiation time was calculated as follows:

$$mW/cm^2 = \frac{mW \times 4}{\pi \times 3.4^2}$$

$$W/cm^2 = \frac{mW/cm^2}{1000}$$

$$Time (s) = \frac{J/cm^2}{W/cm^2}$$

Cells were cultured at a total of 5 x 10⁵ cells per petri dish in complete media. Cultures were divided into 4 study groups. Group 1 was the control and received no irradiation or PS, group 2 contained PS but no irradiation, group 3 was irradiated but no PS was added. Group 4 was treated with AlPcS₄Cl and was irradiated. All samples were incubated for 24 h after PDT treatment followed by biochemical analysis.

2.5.3. Morphology

Any morphological changes of the isolated lung CSCs post PDT treatment were observed and studied using an Olympus CKX41 inverted light microscope (Wirsam, Olympus CKX41) 24 hours post irradiation, whereby changes were captured using the SC30 Olympus camera.

2.5.4. Cytotoxicity

To determine the toxicity induced by PDT. The amount of LDH released from the cells into the culture medium was measured. This determines the amount of cell membrane damage and cell death. This oxidoreductase inter-converts lactate into pyruvate. Its discharge from the cytosol leads to an unusual increase of the enzyme in culture media *in vitro*. Formazan a product of tetrazolium salt conversion through NADH reduction, was measured using a nonradioactive colorimetric assay. The amount of formazan is proportional to the number of cells that have membrane damage and lysed due to undergoing cell death induced by PDT treatment. The CytoTox96® nonradioactive cytotoxicity assay (Promega, G400) was used according to manufacturer specifications. We evaluated cytotoxicity by measuring formazan with a multilabel Counter (Perkin Elmer, VICTOR3™, 1420) at 490 nm.

2.5.5. Proliferation

The effect of PDT on CSC metabolism was determined by measuring the amount of ATP present in the cells after treatment. Intracellular ATP was measured using the CellTiter-Glo® luminescent cell proliferation assay (Promega, G7570) and used according to manufacturer specifications. Luciferase present in the reagent catalyzes the oxidation of luciferin to oxyluciferin and illuminates in the presence of cellular ATP. Luminescence was read and quantified using a Multilabel Counter (Perkin Elmer, VICTOR3™, 1420) expressed in RLU. The amount of luminescence is directly proportional to ATP levels indicative of metabolically active cells. A reduction in luminescence is representative of cell inhibition and cell death induced by the anticancer treatment causing a reduction in intracellular ATP.

2.5.6. Viability

The adjustment in cell numbers because of development restraint instigated by PDT on the CSCs was resolved utilizing the trypan blue viability assay. This color prohibition test permits live (feasible) cells with flawless membranes to bar the color and stay unstained, though dead (non-suitable) cells will hold the color and stain blue. An equivalent volume of cells and 0.4% Trypan blue (Sigma Aldrich, T8154) was homogenously blended and exchanged to a chamber slide which was then embedded into a computerized cell counter (Countess® Automated Cell Counter) which visually delineates the cells and after that electronically calculates the level of viable cells.

2.5.7. Cell Death

Annexin V propidium iodide (PI) was used to measure cell death post irradiation. The assay gives an indication of cell death either as necrotic or apoptotic. The test makes use of fluorescently labelled dyes which are then read using a flow cytometer quantifying the amount of fluorescently labelled cells.

24 Hours after PDT treatment, cells were detached and washed with HBSS. Cells were re-suspended in 1X binding buffer at a concentration of 1×10^6 cells/ml and 100 μ l of the cell suspension was transferred into flow cytometry tubes. Five microliters of each Annexin V-FITC and PI reagents (BD Pharmingen™, 559763) were added and the tubes were thoroughly mixed and incubated for 10 min at room temperature in the dark. Within 1 h, flow cytometric analysis was performed on the BD Flow cytometer (BD Accuri™ C6 Cytometer) and Annexin V-FITC and PI was detected as a green and red fluorescence, respectively.

2.6. Statistics

All experiments were repeated four times. Data processing was done using Sigma plot version 12/13. Error bars are representative of the mean (SEM) ($n = 3$). Data accumulated was statistically evaluated by Student's paired t-test, and the significance was defined as $p < 0.05$ (*), $p < 0.01$ (**) or $p < 0.001$ (***). All colorimetric, luminescent and absorbance assays was performed using a background control that was subtracted from the raw data obtained.

3. Results/ discussion

3.1. Characterization of isolated lung CSCs

CSCs have been isolated from solid tumors and cell lines and their intense ability to initiate tumor formation as well as differentiate upon *in vivo* application has been demonstrated [20]. Studies on how to identify and isolate CSCs have elaborated on the various markers, gene expression molecules and cell signaling pathways involved in CSC research. The most common method applied in identifying and isolating sub populations of cells is through protein marker detection or cluster of differentiation molecules. Over expression of common stem cell genes or markers representative of the tissue of origin has been seen in various stem cells including CSCs. Allowing for identification of stem ness inside a tumor population [21]. One way of differentiating CSCs from non-tumorous stem cells and cancerous cells is that CSCs undergo altered glycosylation during malignant transformation. Giving CSCs cancer specific glycans and their tumorous characteristics of tumor aggressiveness, progression, and metastasis along with increased levels of stem marker expression [22].

After isolation of the subpopulation of stem like cells from the lung cancer cell line A549 using magnetic beads attached to protein markers we had to identify whether the population of cells were of stem cell origin. This was done using CD markers specific to lung CSCs including CD 133, CD 56 and CD 44. The methods used to identify these markers included antibody identification through flow cytometry and IFL staining.

3.1.1. Flow Cytometry

In order to determine whether the cells isolated were of stem cell origin, antigenic detection was assessed using the BD Accuri™ C6 Flow Cytometer. Indirect antibody labelling allowed to fluorescently express whether or not the primary antibody is present on the cells. FL detection using flow cytometry showed that the isolated cells expressed the markers CD 133, CD 44 and CD 56 (Figure 2).

Flow Cytometric characterisation of lung CSCs

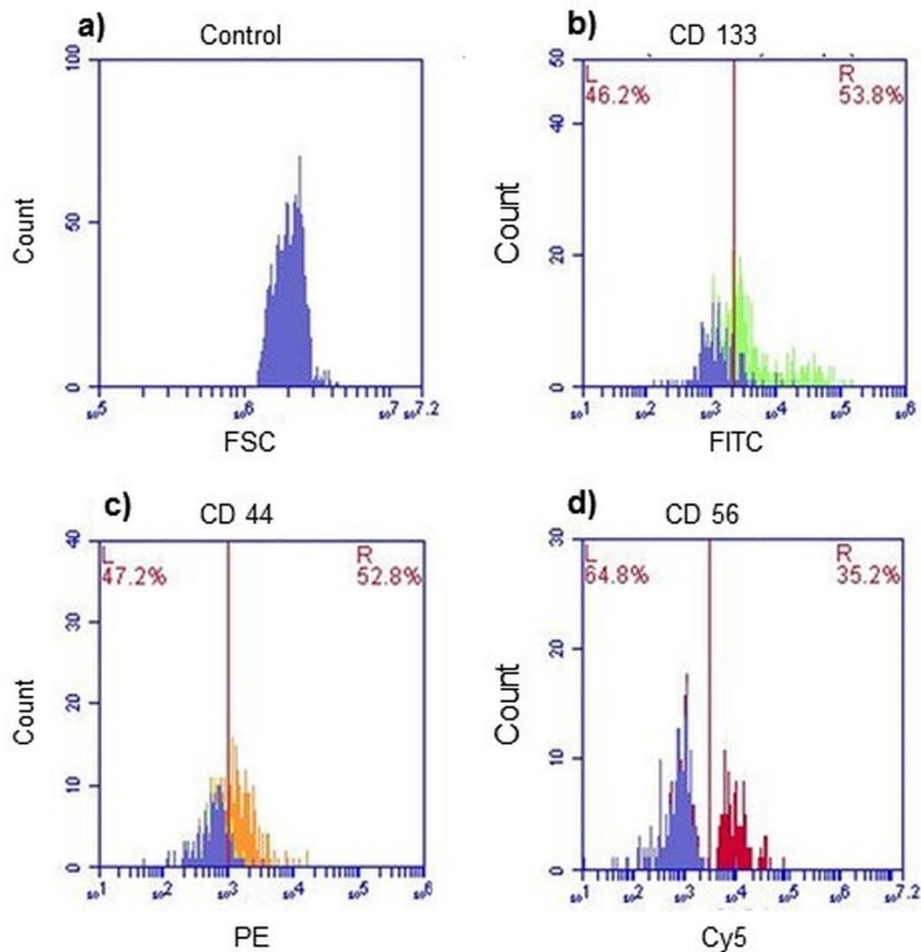


Figure 2. Fluorescence protein detection using flow cytometry. a) Unstained lung CSCs (control). b) Lung CSCs positive for CD 133 (FITC), c) Lung CSCs positive for CD 44 (PE), and Lung CSCs positive for CD 56 (Cy5). All positive samples are overlaid with the control to distinguish between the color shifts.

Analysis of the flow cytometric results was performed by running a control sample in order to establish the population group by gating the cell population on the density plot and expressing it as a blue peak on the histogram (Figure 2 a)). Experimental samples labelled with the primary antigenic markers and fluorophore tags were run and gated and further analyzed for the expression of the respective markers. Cells labelled with, CD 133 was tagged with FITC (green) and fluorescence was detected using FL-1 with a 533/30 filter and 488 nm laser (Figure 2 b)); CD 44 was tagged with PE (orange) and fluorescence detected using FL-2 with a 585/40 filter and 488 nm laser (Figure 2 c)); and CD 56 was tagged with Cy5 (red) and fluorescence detected using FL-3 with a 670 LP filter and 488 nm laser (Figure 2 d)). Results expressing two peaks are indicative of the unstained control population that is overlaid onto the positively stained populations in order to differentiate between the two. Results indicate that the cells isolated are lung CSCs.

3.1.2. Immuno Fluorescence

Expression of the antigenic CSC markers after isolation of the side population was determined by IFL microscopy. Isolated lung CSCs expressed the surface marker CD 133, CD 44 and CD 56. Control cell lines positive for the antigenic markers confirmed the antigenic expression as seen by the fluorescence detected. No fluorescence was observed from the negative control cell lines, indicating that these cells do not express the surface markers. DAPI was used to counterstain the nuclei. Positive expression of the antigenic surface markers confirmed positive isolation of lung CSCs (Figure 3 - 5).

Fluorescent antigenic detection of the surface marker CD 133

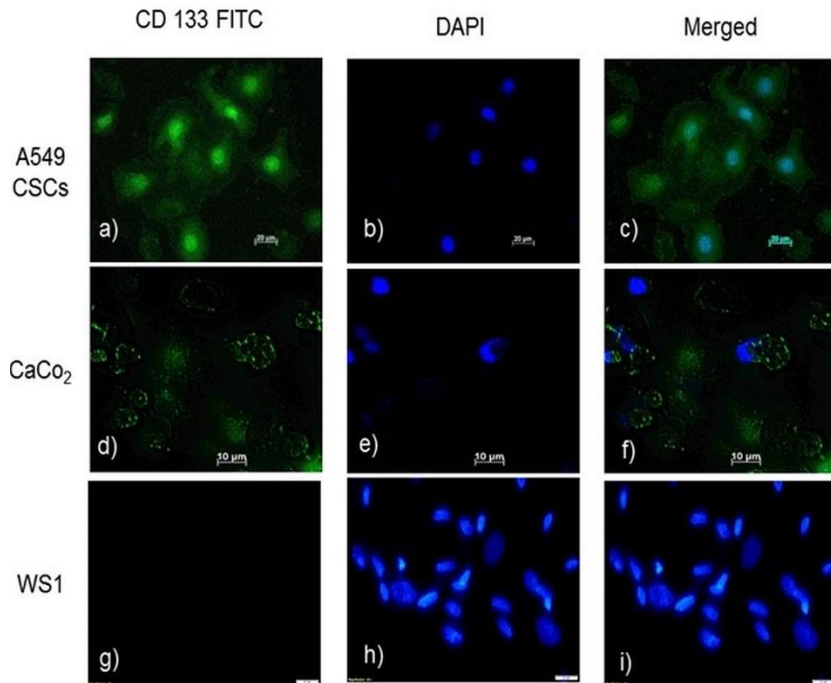


Figure 3. Fluorescent antigenic detection of the surface marker CD 133. Immunofluorescent staining of the isolated side population of Lung CSCs (a) and control cell CaCo₂ (d) positive for the antigenic marker CD 133 indicated positive fluorescence with FITC (green). Negative control cell line WS1 (g) indicated no fluorescence. All cell lines were counter stained with DAPI indicated by blue fluorescence seen in the nuclei (b, e, and h). Merged fluorescent images of the labelled cell lines are indicated by image c, f and i.

Fluorescent antigenic detection of the surface marker CD 44

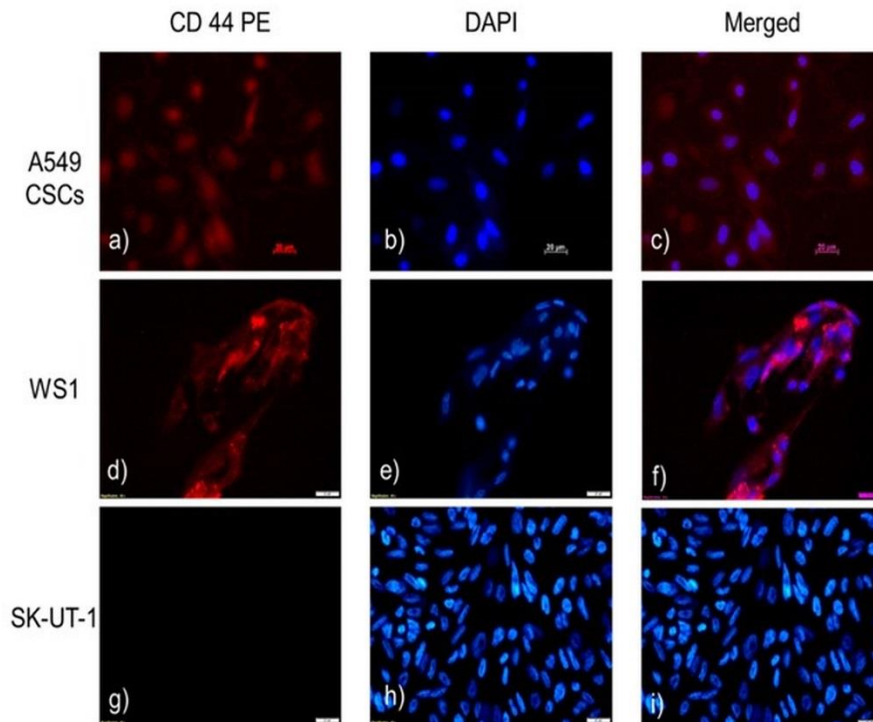


Figure 4. Fluorescent antigenic detection of the surface marker CD 44. Immunofluorescent staining of the isolated side population of Lung CSCs (a) and control cell WS1 (d) positive for the antigenic marker CD 44 indicated positive fluorescence with PE (red). Negative control cell line SK-UT-1 (g) indicated no fluorescence. All cell lines were counter stained with DAPI indicated by blue fluorescence seen in the nuclei (b, e, and h). Merged fluorescent images of the labelled cell lines are indicated by image c, f and i.

Fluorescent antigenic detection of the surface marker CD 56

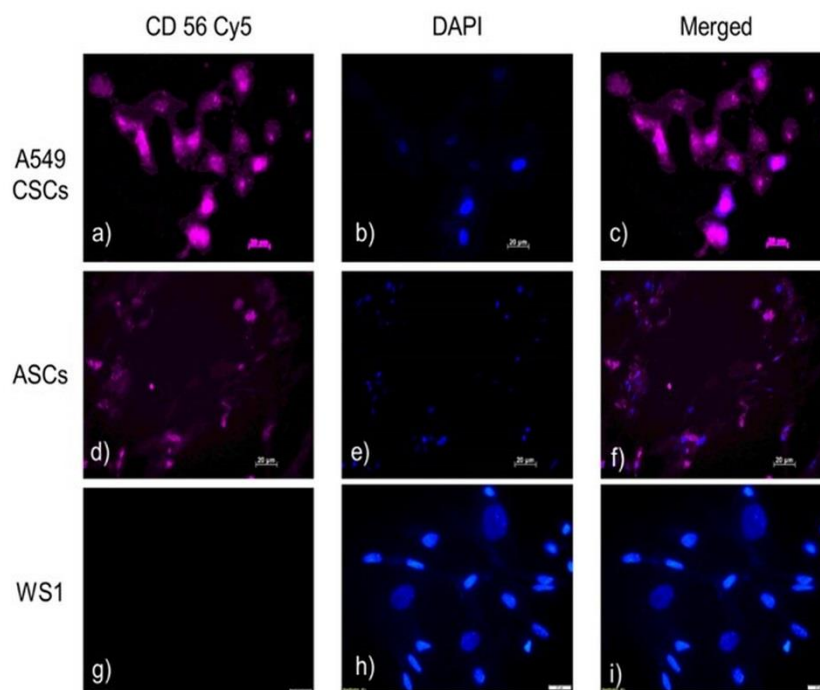


Figure 5. Fluorescent antigenic detection of the surface marker CD 56. Immunofluorescent staining of the isolated side population of Lung CSCs (a) and control cell ASC (d) positive for the antigenic marker CD 56 indicated positive fluorescence with Cy5 (magenta). Negative control cell line WS1 (g) indicated no fluorescence. All cell lines were counter stained with DAPI indicated by blue fluorescence seen in the nuclei (b, e, and h). Merged fluorescent images of the labelled cell lines are indicated by image c, f and i.

3.2. Localization of PS in lung CSCs

The intracellular confinement of a PS is critical to characterize the system and effectiveness of photo actuated cell death. This is expected by PDT following two sorts of components including a type I system where through a redox procedure an energized triplet state PS interface with intracellular targets including film lipids, proteins, DNA and sub-atomic oxygen, framing radicals. Radicals can be oxidized to shape superoxide or associate with oxygen, hydrogen peroxide, redox-dynamic progress metals, nitrogen oxide or redox-dynamic locales of biomolecules framing ROS. Type II system the energized triplet state PS exchanges energy to atomic oxygen framing $^1\text{O}_2$ an exceedingly cytotoxic species. The two ROS and $^1\text{O}_2$ actuate annihilation of biological targets [11]. Mitochondria are associated with cell homeostasis by directing ATP levels just as framing synthetic substances for breakdown of poisons, they contain different atoms including DNA, ribosomes and compounds for protein and phospholipid combination. Focusing on the mitochondria as a PDT target will prompt cell destruction. Lysosomes contain proteins for hydrolysis or processing of biomolecules just as outside particles to help in the expulsion of atoms from the cell. Focusing on lysosomes can prompt downregulation of cell homeostasis and obviously cell death. In order to establish the suitability of AlPcS_4Cl as a PS we determined whether AlPcS_4Cl localizes in intracellular organelles such as mitochondria and lysosomes. This was confirmed using IFL and DIC, where mitochondria and lysosomes were fluorescently labelled using FITC and the PSs' auto fluorescence exploited and detected using FL microscopy (Figure 6 and 7).

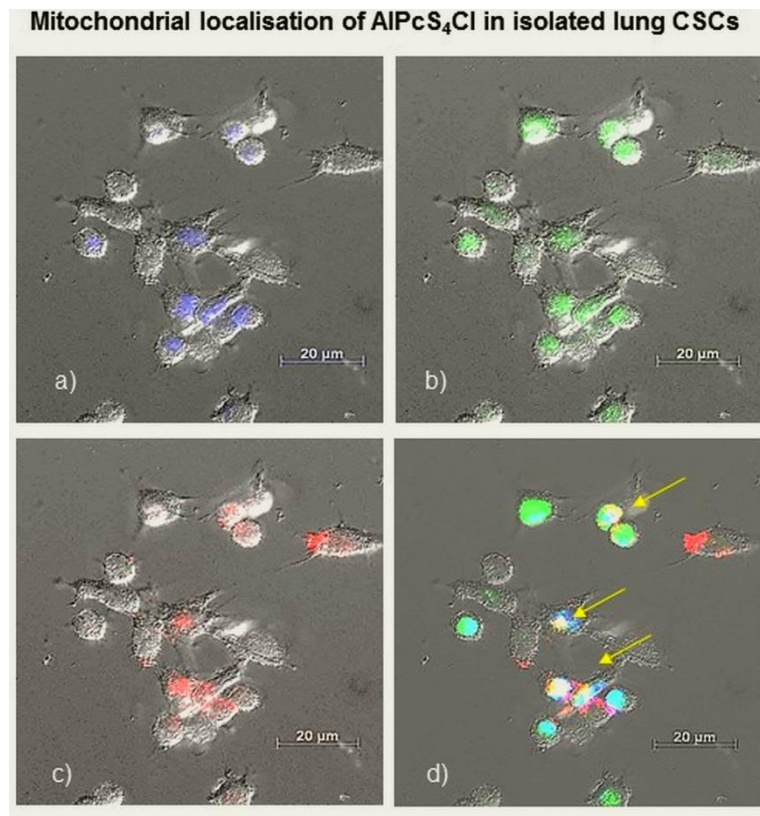


Figure 6. Mitochondrial localization of AIPcS₄Cl in isolated lung CSCs. a) Nuclei are stained blue using DAPI, b) Mitochondria fluoresces green (FITC), c) AIPcS₄Cl auto fluoresces red (Cy5), d) Intermediate yellow is seen in the superimposed images where the green and red channels are merged and fluorescence from the mitochondrion and PS are overlapping.

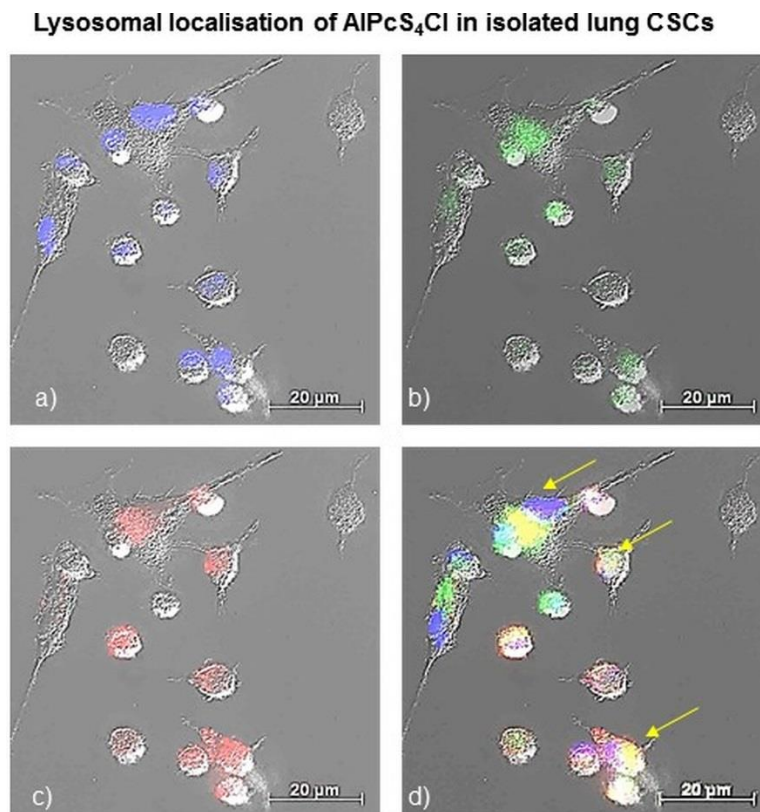


Figure 7. Lysosomal localization of AIPcS₄Cl in isolated lung CSCs. a) Nuclei are stained blue using DAPI, b) Mitochondria fluoresces green (FITC), c) AIPcS₄Cl auto fluoresces red (Cy5), d) Intermediate yellow is seen in the superimposed images where the green and red channels are merged and fluorescence from the lysosomes and PS are overlapping.

Figure 6 and 7 shows the intracellular localization of the PS, where AIPcS₄Cl localizes in the perinuclear area in the mitochondrion as well as the lysosomes of the isolated lung CSCs. The images show superimposed DIC microscopy and FL imaging of a) the nucleus (DAPI - blue), b) mitochondria / lysosomes (FITC - green), c) AIPcS₄Cl- auto fluorescence (Cy 5 - red) and d) a superimposed image of all the fluorescent markers combined. Figure 6 d) and 7 d) shows intracellular localization of AIPcS₄Cl in both the mitochondria and lysosomes depicted by a resultant yellow fluorescence seen when merging the two color channels (FITC and Cy 5), white fluorescence is noted due to all the color channels overlapping, where the primary colors (red, blue and green) result in white, giving an indication that the PS surrounds the perinuclear area. This in turn signifies that organelles involved in cell function and viability will be targeted upon photo activation of AIPcS₄Cl, whereby ROS or ¹O₂ formation and accumulation will destroy these organelles that can lead to CSC death.

3.3. Photodynamic Therapy

In order to determine whether the PS AIPcS₄Cl exerts any responses in isolated lung CSCs an array of biochemical assays were tested along with morphological features. This gives an indication of the extent of PDT damage by assessing post-irradiation cellular phenotypic components.

3.3.1. Morphology

Following PDT on the isolated lung CSCs, the cells were characterized morphologically. All the treatment groups were compared to the respective control sample which did not receive any treatment. The results indicated that the isolated lung CSCs receiving irradiation alone had an increase in cell proliferation indicated by an increase in the monolayer density. This is in accordance with previous studies conducted using photobiomodulation (PBM) of 10 J/cm² and wavelengths ranging from 630 – 830 nm on lung CSCs and various cancer cell lines, having an increase in cell proliferation and viability [23; 24]. Isolated lung CSCs receiving PS at a concentration of 20 μM alone did not indicate changes in morphology when compared to its respective control. The cells presented with a dense monolayer of cells that are viable with no membrane damage or signs of cytotoxicity. Thus indicating the safety of using AIPcS₄Cl as a PS [25; 26]. CSCs that received PDT treatment showed alterations in morphology. Cell death due to intrinsic apoptosis was noted, where changes included cell shrinkage, chromatin condensation, cell blebbing and cytoplasmic vacuolization; and programmed necrosis, indicated by cell swelling and lysis (Figure 8).

Morphology of Isolated Lung CSCs post PDT

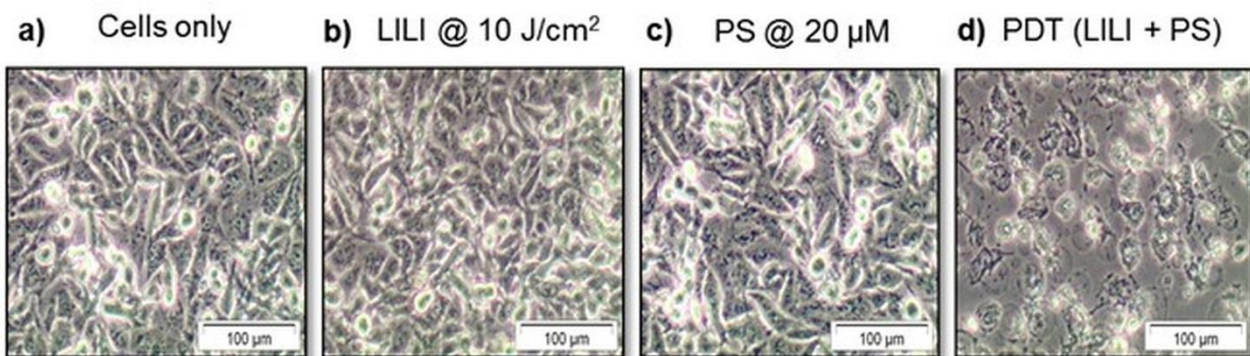


Figure 8. Morphology of Isolated Lung CSCs post PDT. Cells only represent healthy viable lung CSCs. CSCs receiving LILI with an energy of 10 J/cm² indicated an increase in cell proliferation, seen by an increase in the cell monolayer density when compared to the density of the control sample. No cytotoxic morphological changes are seen in lung CSCs after receiving AIPcS₄Cl of 20 μM without photo activation. Cellular morphology resemble that of the control sample receiving no PS. Lung CSCs that received PDT with a 20 μM AIPcS₄Cl concentration activated using 10J/cm² irradiation, show indications of cell death, following an apoptotic and necrotic pathway.

3.3.2. Cytotoxicity

To explore the PDT activity of AIPcS₄Cl on isolated lung CSCs, a series of LDH cytotoxicity assays were performed. Results seen in Figure 9 indicated that there was no significant cytotoxicity associated with exposure to light irradiation alone in the absence of the PS. This result is due to red photobiomodulation which is used at a low power and low fluence output having a bio stimulatory effect on cells [27; 28], thus having no indication of cytotoxicity. The results seen from

the group treated with PS alone in the absence of excitation light had shown no significant cytotoxicity. One of the characteristics of an ideal PS is to have negligent dark toxicity [29], which was seen when using AIPcS₄Cl [26]. A significant increase in cytotoxicity was observed in CSCs receiving both PS and LILI/ PDT treatment. In order to establish the percentage of cytotoxicity induced a positive control sample was used, whereby the cells were completely lysed prior to running LDH cytotoxicity assays using the cell lysates in the culture media. The positive control sample represents 100 percent (%) cytotoxicity. The percentage cytotoxicity achieved using PDT with AIPcS₄Cl on isolated lung CSCs were seen to be 36.13 % when using 20 μ M AIPcS₄Cl and 10 J/cm² LILI.

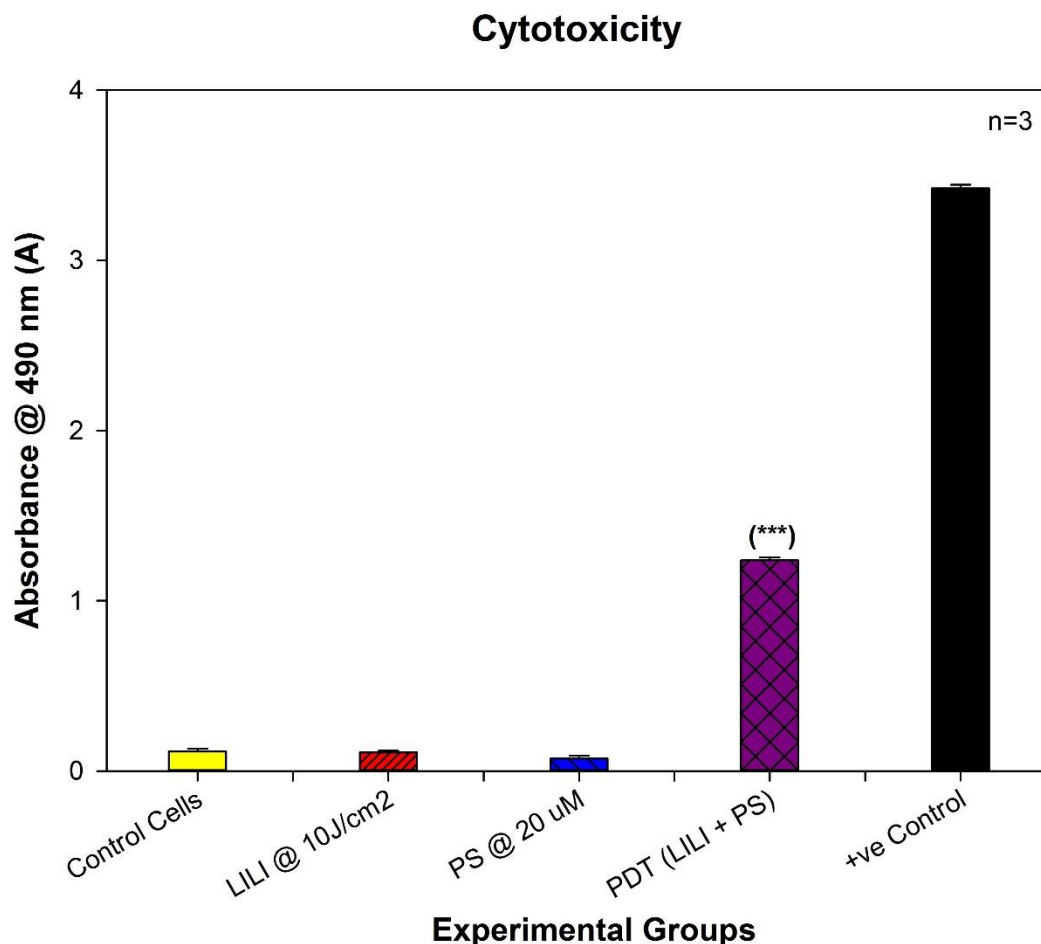


Figure 9. LDH Cytotoxicity of Isolated Lung CSCs post PDT. Cytotoxicity was measured as an absorbance value @ 490 nm. All test samples were compared to their respective control cells. No statistical significance was seen when exposing the cells to PS or LILI alone. A statistical significance of $p < 0.001$ in LDH cytotoxicity was observed when treating the cells with PDT using 20 μ M AIPcS₄Cl and 10 J/cm² LILI, which was calculated as a percentage value in comparison to the positive control sample representing 100 %. The percentage cytotoxicity achieved in isolated lung CSCs was 36.13 %.

3.3.3. Proliferation

All metabolically active cells require energy in order to perform cellular processes such as proliferation. Most cancerous cells produce ATP energy through aerobic glycolysis [30]. To determine whether PDT had an effect on isolated lung CSCs, we measured the amount of ATP present in the test samples in order to determine what amount of ATP is present in metabolically functional lung CSCs and whether PDT reduces cellular processes, which can be seen by a decrease in intracellular ATP measured. Proliferation results (Figure 10) indicate that cells treated with LILI and PS only, had no significant impact when compared to their control cells receiving no treatment. Although previous studies established that LILI at wavelengths between 630 nm and 800 nm using low energy densities of 10 J/cm² had a proliferatory effect on various cell lines [31-33], it was noted that LILI had no significant effect on lung CSCs. This is in accordance with research stating that CSCs or stem cells have a decreased or quiescent metabolism [34], which ultimately impacts the metabolic rate and the effect LILI has on lung CSCs, also considering the fluence and wavelength used to irradiate the cells. Due to AIPcS₄Cl's negligent dark toxicity, it is noted that the CSCs receiving only PS had a similar metabolic rate as its control cells, due to the PS having no effect in its un-activated state. Lung CSCs that was treated with PDT showed a significant decrease in cell metabolism, seen by a decrease in ATP luminescence. Indicating

when using 20 μM AIPcS₄Cl and 10 J/cm² LILI, it can significantly decrease the proliferation rate of lung CSCs and lead to CSC death *in vitro*.

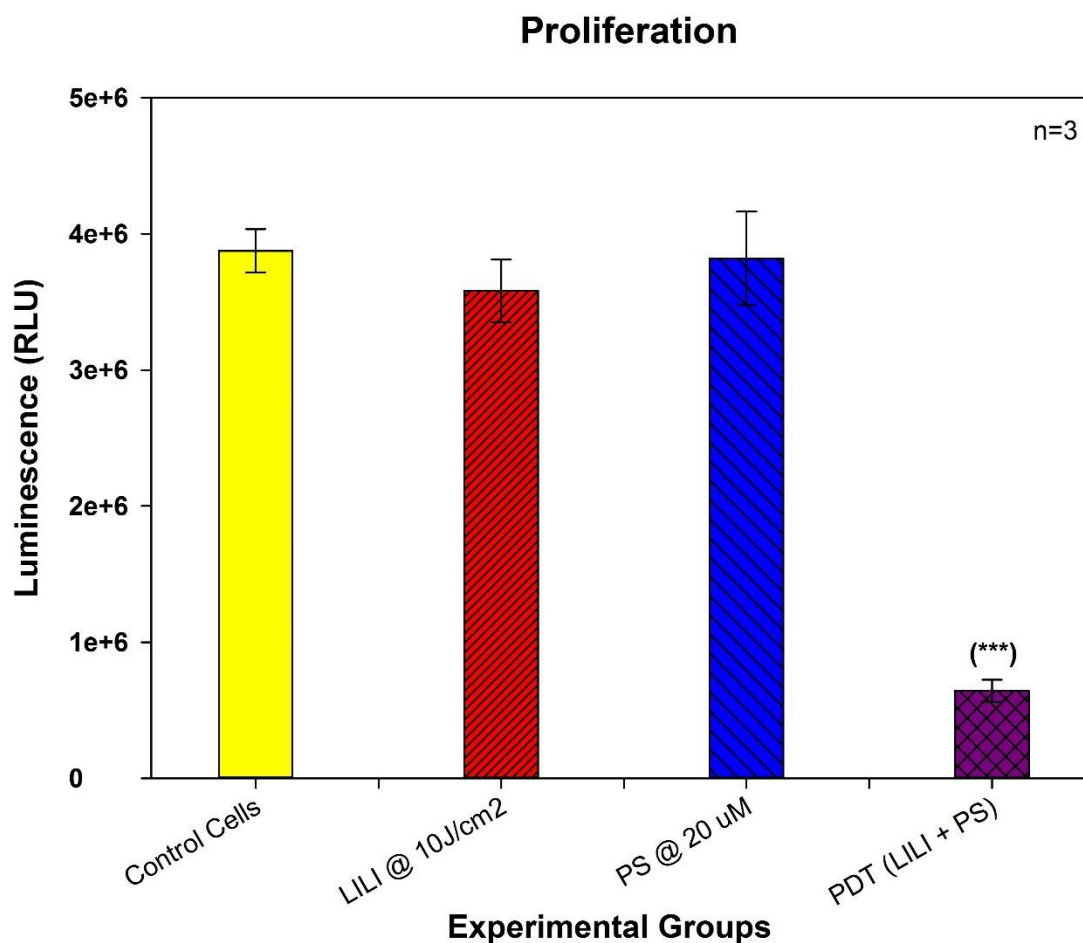


Figure 10. ATP Proliferation of Isolated Lung CSCs post PDT. ATP was measured as a luminescent value in relative light units (RLU). All test samples were compared to their respective control cells. No statistical significance was seen when exposing the cells to PS or LILI alone. A statistical significant decrease in ATP proliferation of $p < 0.001$ was observed when treating the cells with PDT using 20 μM AIPcS₄Cl and 10 J/cm² LILI.

3.3.4. Viability

Trypan Blue exclusion assay is a well-established method for identifying viable and dead cells, as it reflects the viability based on cell membrane integrity [35]. Viable cells that have not undergone any stress induction will exclude the dye. Whereas cells exposed to treatments or environmental factors inducing stress, whereas in the case of PDT ROS mediated cytodamage, will have diminished cell membrane integrity, permeable to the dye, indicative of cell death. This method permits us to establish the effect PDT has on isolated lung CSC viability. Results were recorded as a percentage value of the proportion of viable cells after experimental treatment as seen in Figure 11. The results show that there is no significant difference in viability in CSCs treated with LILI and PS alone, as compared to the control sample. Confirming that LILI at 10 J/cm² does not have a significant stimulatory action on lung CSCs, as well as AIPcS₄Cl having no dark toxicity when exposing the cells to the PS without light activation. There is however a significant decrease seen in viability after PDT treatment of the lung CSCs. This is indicated by a 46 % decrease in viability as compared to the respective control cells.

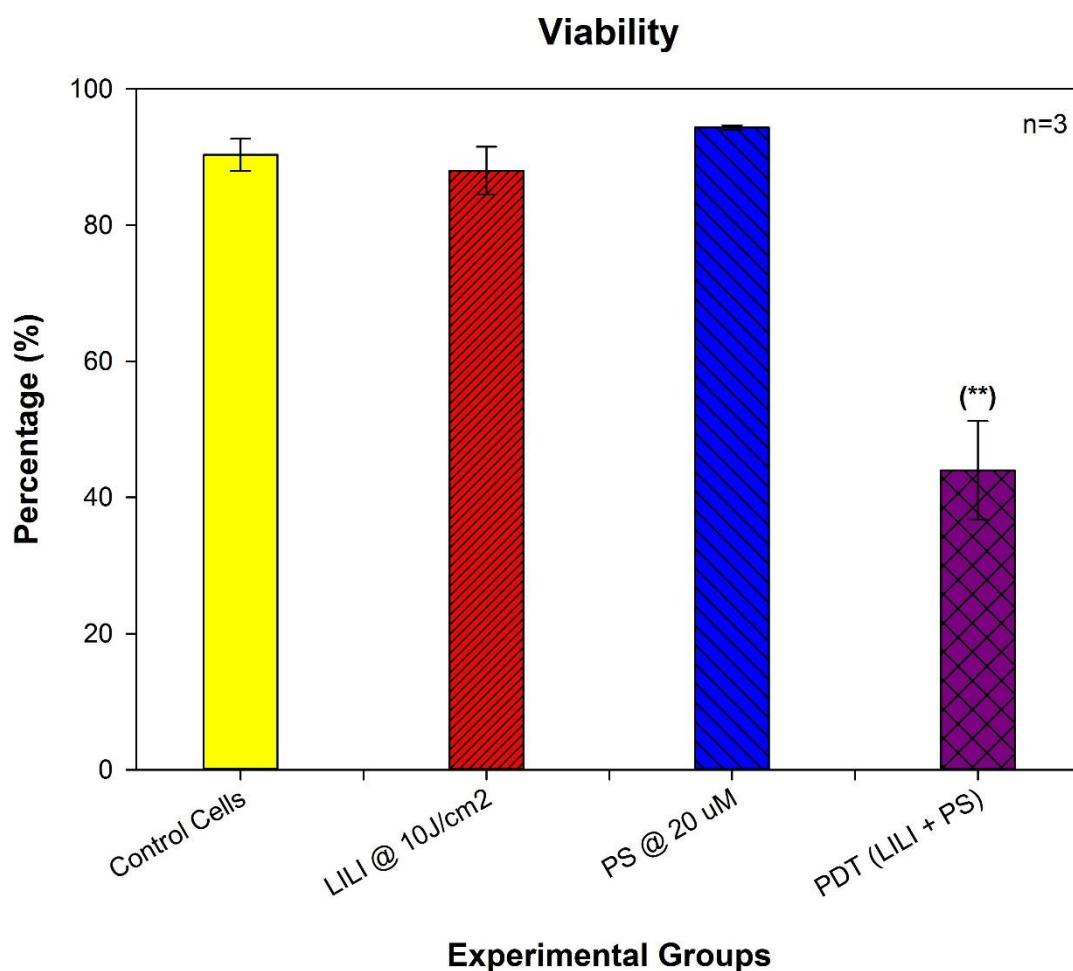


Figure 11. Trypan Blue Viability of Isolated Lung CSCs post PDT. Trypan Blue was used as a dye exclusion assay, where viable cells excluding the dye was recorded as a percentage value. All test samples were compared to their respective control cells. No statistical significance was seen when exposing the cells to PS or LILI alone. A statistical significant decrease ($p < 0.01$) in viability of 46 % was seen when treating the cells with PDT using 20 μM AlPcS_4Cl and 10 J/cm^2 LILI, when compared to the respective control samples.

3.3.5. Cell death

It has been established that PDT directly destroys cancer cells by inducing either apoptotic or necrotic cell death where these mechanisms can occur concurrently [36]. Photodynamic induced cell death is seen due to the formation of ROS associated with oxidative stress and subsequent cell damage by oxidizing and degrading cell components [37]. In order to establish whether PDT induced apoptotic or necrotic cell death in isolated lung CSCs, an Annexin V PI cell death assay was done. In apoptotic cells, phosphatidylserine is translocated from the internal to the external part of the plasma membrane, exposing phosphatidylserine, making it available for Annexin V a phospholipid binding protein to attach to it [38]. Phosphatidylserines' translocation is an initial occurrence preceding the loss of membrane integrity associated with later cell death pathways. For this reason propidium iodide (PI) is used in conjunction with Annexin V, as a nucleic acid intercalator that penetrates porous cell membranes, enabling it to attach to DNA. Making it possible to distinguish between cells that are viable, cells that are in early apoptosis, late apoptosis and necrotic [39]. Flow cytometric results (Figure 12) show that PDT does induce apoptosis and necrosis in lung CSCs. This was established by running an unstained sample of cells to determine the cell population. A sample of lung CSCs where apoptosis was induced using hydrogen peroxide as a positive control to establish apoptotic events and the control cell sample with no PS or LILI along with cells receiving PS alone or LILI alone which showed no significant cell death. Whereas lung CSCs treated with PDT indicated statistical significant ($p < 0.001$) increases in early apoptotic, late apoptotic and necrotic cell death.

Cell Death – Annexin V PI

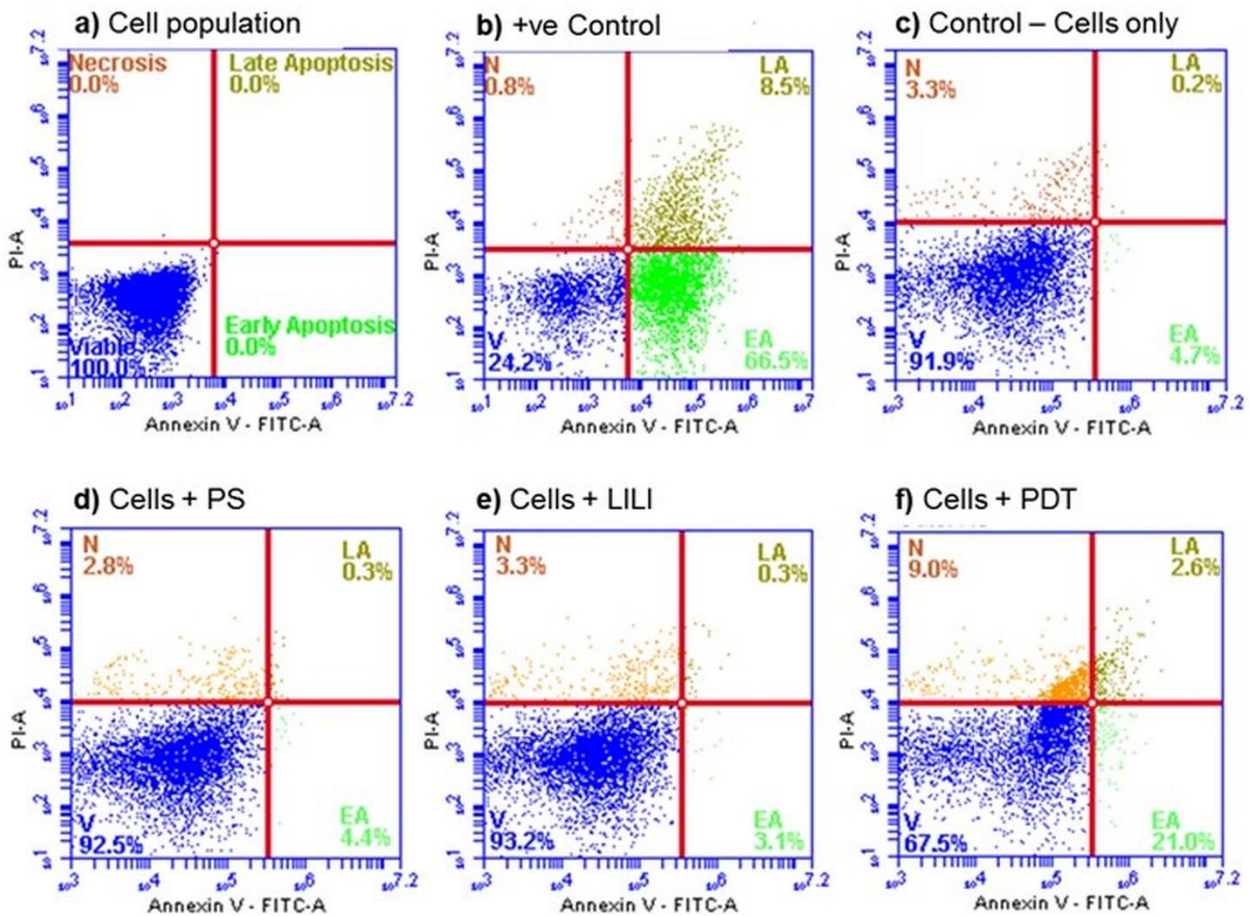


Figure 12. Cell Death – Annexin VPI of Isolated Lung CSCs post PDT. Unstained cells were used to establish the cell population (a). A positive control sample was used where apoptosis was induced using hydrogen peroxide (b). Cells receiving no treatment was used as the control (c). Cells receiving PS or LILI alone had no significant cell death with viabilities of 92.5 % and 93.2 % respectively (d – e). Cells receiving PDT showed a statistical significant increase ($p < 0.001$) in early apoptosis (21 %), late apoptosis (2.6 %) and necrosis (9 %).

At present, PDT using different types of PSs, has proven effective in treating most solid tumors both *in vitro* and *in vivo*. Although the outcomes of PDT on isolated lung CSCs have yet to be elucidated until now. In this study we elaborated on the effects that PDT using AlPcS₄Cl has on isolated lung CSCs in order to establish its treatment potential for lung cancer. Morphologic and biochemical assessments were performed on several groups of isolated lung CSCs displaying stem like markers including CD 133, CD 44 and CD 56 all of which has been identified to promote cancer recurrence and metastasis. Where CD 133 is the most frequently found CSC marker. This cell surface glycoprotein aids in self-renewal, tumor initiation and drug resistance where it has been shown to maintain cancer stem-like and chemo, radio resistant properties in lung cancer derived CD 133+ cells [40]. CD 44 has been reported to be associated with poor prognosis of lung cancer, where it has been established that lung cancer cell lines that are CD 44+ had increased proliferative and colony forming potential [41]. Neural cell adhesion molecule CD 56 has been reported to be highly expressed in cases of lung cancer recurrence, where this marker has been established as a diagnostic tool for lung cancer as well a potential target for drug immuno-therapy [42]. Due to the severity of tumorigenic potential seen when lung CSCs express these markers we used them as a treatment population in our experiment. The lung CSCs were effectively isolated using magnetic cell sorting and characterized by IFL and flow cytometric protein detection.

The PS chosen for this study, AlPcS₄Cl, was used due to its preferential features for a successful PS, demonstrated by its photo stability and amphipathic nature, negligent toxicity in the dark, localizes in intracellular organelles that upon membrane damage and ROS formation cause apoptotic cell death and its activation wavelength which is optimal for tissue penetration [26]. Results confirmed that the intracellular confinement of this PS in lung CSCs are optimal for cell death induction via apoptosis. This was seen where the PS localizes in intracellular organelles that upon photo activation will result in the production of ROS and free radicals which will ultimately destroy these cellular structures inhibiting their functions leading to cell death.

PDT treatment of the lung CSCs was arranged in several treatment groups where the control group consisted of cells not exposed to either variables including irradiation or PS, ruling out possible effects not indicated by PDT. Similarly a group of cells received PS alone and LILI alone, whereby the influence of the PS in its inactive state could be measured and the effect of LILI in the absence of a PS was evaluated. Results indicated that neither individual components induced any significant changes to the lung CSCs, However, PDT had significant changes when analyzing the morphological and biochemical assessments. Changes in morphology were in accordance with those seen induced by apoptosis caused by the activated PS forming cytotoxic species that interact with cellular components causing the observed cell damages. Morphological results were confirmed by LDH cytotoxicity, which quantifies enzymes released into the culture medium upon cell destruction. Results indicated a significant increase in LDH cytotoxicity. Results were further corroborated by ATP proliferation and Trypan Blue viability analysis showing a significant decrease in CSC proliferation and viability as compared to the control samples. When comparing results to those established in a previous study using a similar PS and laser parameters on lung cancer cells it was noted that the amount of cytotoxicity achieved was higher in lung CSCs than lung cancer alone. Similarly the findings showed a greater decrease in proliferation for CSCs than lung cancer, viability comparisons indicated a similar result in viability of $\pm 43\%$ [26]. Further validating the above mentioned findings was cell death analysis using Annexin V PI, confirming cell death via apoptosis and necrosis. This would suggest that AIPcS₄Cl show a desired effect when used on lung CSCs as a photodynamic drug.

4. Conclusion

Lately, CSCs have been identified in numerous tumors and have been proposed to explain metastatic capacity, recurrence, and resistance to radiotherapy and chemotherapy that some tumors poses. Research suggest that tumors contain a small subpopulation of cells that can self-renew, proliferate infrequently, express several pluripotency genes and are responsible for tumor initiation and metastasis [43]. Anticancer agents that destroy highly proliferative tumor cells do not affect CSCs, therefore treatments need to destroy CSCs in particular to eradicate the tumor. CSCs that evade cancer therapy will be responsible for tumor drug resistance and relapse. Stem cell markers have been associated with CSCs that can be used to isolate and enrich a population of cells displaying these stem cell markers [44]. CSCs can be identified and isolated using different approaches including flow cytometry and magnetic-associated cell sorting. This study proves that PDT using AIPcS₄Cl has the desired effects of killing lung CSCs. This is seen in morphological features of apoptosis and necrosis that included cell shrinkage, chromatin condensation, cell blebbing, cytoplasmic vacuolization and cell swelling and lysis. Furthermore, results on cell toxicity, proliferation, viability and cell death corroborated these morphological findings, where AIPcS₄Cl-PDT caused a significant increase in cytotoxicity, and significant decreases in cell proliferation and viability, as well as cell death analysis presenting significant increases in early-, late-apoptosis and necrosis. It should be mentioned that PDT can be considered as a palliative treatment along with established lung cancer therapies, which can enhance the prognostic outcome of the treatments by killing of CSCs. Photodynamic anticancer therapy is aimed at destroying cancerous cells alone, preserving normal cells [45]. Therefore the effects of the particular PS need to be explored on normal lung cells.

5. Conflict of interest

The authors declare no conflict of interest

6. Acknowledgements / Funding

This work is based on the research supported by the South African Research Chairs Initiative of the Department of Science and Technology and National Research Foundation of South Africa (Grant No 98337). The authors sincerely thank the University of Johannesburg and the National Laser Centre – Council for Scientific and Industrial Research South Africa (CSIR) for their facilities and laser equipment and the National Research Foundation of South Africa (SARChI-DST) for their financial grant support.

7. References

- [1] Colditz, G. A., & Wei, E. K. (2012). Preventability of cancer: The relative contributions of biologic and social and physical environmental determinants of cancer mortality. *Annual Review of Public Health*, 33(1), 137-156. doi: 10.1146/annurev-publhealth-031811-124627.
- [2] Salem, M. S. Z. (2015). Cancer: Some genetic considerations. *Egyptian Journal of Medical Human Genetics*, 16(1), 1-10. doi: <https://doi.org/10.1016/j.ejmhg.2014.09.003>.
- [3] Crous, A., & Abrahamse, H. (2018). Targeted photodynamic therapy for improved lung cancer treatment. In Torres, A. F. C. (Ed.), *Lung cancer*: IntechOpen.
- [4] Lemjabbar-Alaoui, H., Hassan, O. U., Yang, Y.-W., & Buchanan, P. (2015). Lung cancer: Biology and treatment options. *Biochimica et biophysica acta*, 1856(2), 189-210. doi: 10.1016/j.bbcan.2015.08.002.

- [5] MacDonagh, L., Gray, S. G., Breen, E., Cuffe, S., Finn, S. P., O'Byrne, K. J., & Barr, M. P. (2016). Lung cancer stem cells: The root of resistance. *Cancer Lett*, 372(2), 147-156. doi: <https://doi.org/10.1016/j.canlet.2016.01.012>.
- [6] Kreso, A., & Dick, J. E. (2014). Evolution of the cancer stem cell model. *Cell Stem Cell*, 14(3), 275-291. doi: [10.1016/j.stem.2014.02.006](https://doi.org/10.1016/j.stem.2014.02.006).
- [7] Sleeman, J., & Steeg, P. S. (2010). Cancer metastasis as a therapeutic target. *European Journal of Cancer*, 46(7), 1177-1180. doi: <https://doi.org/10.1016/j.ejca.2010.02.039>.
- [8] Eun, K., Ham, S. W., & Kim, H. (2017). Cancer stem cell heterogeneity: Origin and new perspectives on csc targeting. *BMB reports*, 50(3), 117-125. doi: [10.5483/BMBRep.2017.50.3.222](https://doi.org/10.5483/BMBRep.2017.50.3.222).
- [9] Arruebo, M., Vilaboa, N., Sáez-Gutierrez, B., Lambea, J., Tres, A., Valladares, M., & González-Fernández, A. (2011). Assessment of the evolution of cancer treatment therapies. *Cancers*, 3(3), 3279-3330. doi: [10.3390/cancers3033279](https://doi.org/10.3390/cancers3033279).
- [10] Kwiatkowski, S., Knap, B., Przystupski, D., Saczko, J., Kedzierska, E., Knap-Czop, K., Kotlinska, J., Michel, O., Kotowski, K., & Kulbacka, J. (2018). Photodynamic therapy - mechanisms, photosensitizers and combinations. *Biomed Pharmacother*, 106, 1098-1107. doi: [10.1016/j.biopha.2018.07.049](https://doi.org/10.1016/j.biopha.2018.07.049).
- [11] Usacheva, M., Swaminathan, S. K., Kirtane, A. R., & Panyam, J. (2014). Enhanced photodynamic therapy and effective elimination of cancer stem cells using surfactant-polymer nanoparticles. *Mol Pharm*, 11(9), 3186-3195. doi: [10.1021/mp5003619](https://doi.org/10.1021/mp5003619).
- [12] Plaetzer, K., Krammer, B., Berlanda, J., Berr, F., & Kiesslich, T. (2009). Photophysics and photochemistry of photodynamic therapy: Fundamental aspects. *Lasers Med Sci*, 24(2), 259-268. doi: [10.1007/s10103-008-0539-1](https://doi.org/10.1007/s10103-008-0539-1).
- [13] Muehlmann, L. A., Ma, B. C., Longo, J. P., Almeida Santos Mde, F., & Azevedo, R. B. (2014). Aluminum-phthalocyanine chloride associated to poly(methyl vinyl ether-co-maleic anhydride) nanoparticles as a new third-generation photosensitizer for anticancer photodynamic therapy. *Int J Nanomedicine*, 9, 1199-1213. doi: [10.2147/ijn.s57420](https://doi.org/10.2147/ijn.s57420).
- [14] Amin, R. M., Hauser, C., Kinzler, I., Rueck, A., & Scalfi-Happ, C. (2012). Evaluation of photodynamic treatment using aluminum phthalocyanine tetrasulfonate chloride as a photosensitizer: New approach. *Photochem Photobiol Sci*, 11(7), 1156-1163. doi: [10.1039/c2pp05411f](https://doi.org/10.1039/c2pp05411f).
- [15] Sekkat, N., Bergh, H. v. d., Nyokong, T., & Lange, N. (2012). Like a bolt from the blue: Phthalocyanines in biomedical optics. *Molecules*, 17(1), 98.
- [16] Thomas. (1990). Phthalocyanine research and applications.
- [17] Berg, K., Bommer, J. C., & Moan, J. (1989). Evaluation of sulfonated aluminum phthalocyanines for use in photochemotherapy. Cellular uptake studies. *Cancer Lett*, 44(1), 7-15.
- [18] Vrouenraets, M. B., Visser, G. W., Stigter, M., Oppelaar, H., Snow, G. B., & van Dongen, G. A. (2002). Comparison of aluminium (iii) phthalocyanine tetrasulfonate- and meta-tetrahydroxyphenylchlorin-monoconal antibody conjugates for their efficacy in photodynamic therapy in vitro. *Int J Cancer*, 98(5), 793-798.
- [19] Crous, A., Kumar, S. S. D., & Abrahamse, H. (2019). Effect of dose responses of hydrophilic aluminium (iii) phthalocyanine chloride tetrasulphonate based photosensitizer on lung cancer cells. *Journal of Photochemistry and Photobiology B: Biology*. doi: <https://doi.org/10.1016/j.jphotobiol.2019.03.018>.
- [20] Chen, K., Huang, Y.-h., & Chen, J.-l. (2013). Understanding and targeting cancer stem cells: Therapeutic implications and challenges. *Acta Pharmacologica Sinica*, 34, 732. doi: [10.1038/aps.2013.27](https://doi.org/10.1038/aps.2013.27).
- [21] Khan, M. I., Czarnecka, A. M., Helbrecht, I., Bartnik, E., Lian, F., & Szczylik, C. (2015). Current approaches in identification and isolation of human renal cell carcinoma cancer stem cells. *Stem cell research & therapy*, 6(1), 178-178. doi: [10.1186/s13287-015-0177-z](https://doi.org/10.1186/s13287-015-0177-z).
- [22] Barkeer, S., Chugh, S., Batra, S. K., & Ponnusamy, M. P. (2018). Glycosylation of cancer stem cells: Function in stemness, tumorigenesis, and metastasis. *Neoplasia (New York, N.Y.)*, 20(8), 813-825. doi: [10.1016/j.neo.2018.06.001](https://doi.org/10.1016/j.neo.2018.06.001).
- [23] Crous, A., & Abrahamse, H. (2016). Low-intensity laser irradiation at 636 nm induces increased viability and proliferation in isolated lung cancer stem cells. *Photomed Laser Surg*, 34(11), 525-532. doi: [10.1089/pho.2015.3979](https://doi.org/10.1089/pho.2015.3979).
- [24] Kiro, N. E., Hamblin, M. R., & Abrahamse, H. (2017). Photobiomodulation of breast and cervical cancer stem cells using low-intensity laser irradiation. *Tumour Biol*, 39(6), 1010428317706913. doi: [10.1177/1010428317706913](https://doi.org/10.1177/1010428317706913).

- [25] Rocha, M. S., Lucci, C. M., Longo, J. P., Galera, P. D., Simioni, A. R., Lacava, Z. G., Tedesco, A. C., & Azevedo, R. B. (2012). Aluminum-chloride-phthalocyanine encapsulated in liposomes: Activity against naturally occurring dog breast cancer cells. *J Biomed Nanotechnol*, 8(2), 251-257.
- [26] Crous, A., Dhilip Kumar, S. S., & Abrahamse, H. (2019). Effect of dose responses of hydrophilic aluminium (iii) phthalocyanine chloride tetrasulphonate based photosensitizer on lung cancer cells. *J Photochem Photobiol B*, 194, 96-106. doi: 10.1016/j.jphotobiol.2019.03.018.
- [27] Wang, Y., Huang, Y.-Y., Wang, Y., Lyu, P., & Hamblin, M. R. (2017). Red (660 nm) or near-infrared (810 nm) photobiomodulation stimulates, while blue (415 nm), green (540 nm) light inhibits proliferation in human adipose-derived stem cells. *Scientific Reports*, 7(1), 7781. doi: 10.1038/s41598-017-07525-w.
- [28] Crous, A. M. (2016). Photobiomodulatory effects of low intensity laser irradiation on isolated lung cancer stem cells.
- [29] Kiesslich, T., Gollmer, A., Maisch, T., Berneburg, M., & Plaetzer, K. (2013). A comprehensive tutorial on in vitro characterization of new photosensitizers for photodynamic antitumor therapy and photodynamic inactivation of microorganisms. *BioMed research international*, 2013, 840417-840417. doi: 10.1155/2013/840417.
- [30] Vander Heiden, M. G., Cantley, L. C., & Thompson, C. B. (2009). Understanding the warburg effect: The metabolic requirements of cell proliferation. *Science (New York, N.Y.)*, 324(5930), 1029-1033. doi: 10.1126/science.1160809.
- [31] Ziago, E. K., Fazan, V. P., Iyomasa, M. M., Sousa, L. G., Yamauchi, P. Y., da Silva, E. A., Borie, E., Fuentes, R., & Dias, F. J. (2017). Analysis of the variation in low-level laser energy density on the crushed sciatic nerves of rats: A morphological, quantitative, and morphometric study. *Lasers Med Sci*, 32(2), 369-378. doi: 10.1007/s10103-016-2126-1.
- [32] Ayuk, S. M., & Abrahamse, H. (2018). Photobiomodulation alters matrix protein activity in stressed fibroblast cells in vitro. 11(3). doi: 10.1002/jbio.201700127.
- [33] Fekrazad, R., Asefi, S., Allahdadi, M., & Kalhori, K. A. (2016). Effect of photobiomodulation on mesenchymal stem cells. *Photomed Laser Surg*, 34(11), 533-542. doi: 10.1089/pho.2015.4029.
- [34] Peiris-Pagès, M., Martinez-Outschoorn, U. E., Pestell, R. G., Sotgia, F., & Lisanti, M. P. (2016). Cancer stem cell metabolism. *Breast cancer research : BCR*, 18(1), 55-55. doi: 10.1186/s13058-016-0712-6.
- [35] Strober, W. (2001). Trypan blue exclusion test of cell viability. *Curr Protoc Immunol*, Appendix 3, Appendix 3B. doi: 10.1002/0471142735.ima03bs21.
- [36] Yoo, J. O., & Ha, K. S. (2012). New insights into the mechanisms for photodynamic therapy-induced cancer cell death. *Int Rev Cell Mol Biol*, 295, 139-174. doi: 10.1016/b978-0-12-394306-4.00010-1.
- [37] Mfouo-Tynga, I., & Abrahamse, H. (2015). Cell death pathways and phthalocyanine as an efficient agent for photodynamic cancer therapy. *Int J Mol Sci*, 16(5), 10228-10241. doi: 10.3390/ijms160510228.
- [38] Demchenko, A. P. (2013). Beyond annexin v: Fluorescence response of cellular membranes to apoptosis. *Cytotechnology*, 65(2), 157-172. doi: 10.1007/s10616-012-9481-y.
- [39] Rieger, A. M., Nelson, K. L., Konowalchuk, J. D., & Barreda, D. R. (2011). Modified annexin v/propidium iodide apoptosis assay for accurate assessment of cell death. *Journal of visualized experiments : JoVE*(50), 2597. doi: 10.3791/2597.
- [40] Chen, Y. C., Hsu, H. S., Chen, Y. W., Tsai, T. H., How, C. K., Wang, C. Y., Hung, S. C., Chang, Y. L., Tsai, M. L., Lee, Y. Y., Ku, H. H., & Chiou, S. H. (2008). Oct-4 expression maintained cancer stem-like properties in lung cancer-derived cd133-positive cells. *PLoS One*, 3(7), e2637. doi: 10.1371/journal.pone.0002637.
- [41] Hu, B., Ma, Y., Yang, Y., Zhang, L., Han, H., & Chen, J. (2018). Cd44 promotes cell proliferation in non-small cell lung cancer. *Oncology letters*, 15(4), 5627-5633. doi: 10.3892/ol.2018.8051.
- [42] Teicher, B. A. (2014). Targets in small cell lung cancer. *Biochemical Pharmacology*, 87(2), 211-219. doi: <https://doi.org/10.1016/j.bcp.2013.09.014>.
- [43] Chang, J. C. (2016). Cancer stem cells: Role in tumor growth, recurrence, metastasis, and treatment resistance. *Medicine (Baltimore)*, 95(1 Suppl 1), S20-25. doi: 10.1097/md.0000000000004766.
- [44] Phi, L. T. H., Sari, I. N., Yang, Y.-G., Lee, S.-H., Jun, N., Kim, K. S., Lee, Y. K., & Kwon, H. Y. (2018). Cancer stem cells (cscs) in drug resistance and their therapeutic implications in cancer treatment. *Stem cells international*, 2018, 5416923-5416923. doi: 10.1155/2018/5416923.

[45] Agostinis, P., Berg, K., Cengel, K. A., Foster, T. H., Girotti, A. W., Gollnick, S. O., Hahn, S. M., Hamblin, M. R., Juzeniene, A., Kessel, D., Korbelik, M., Moan, J., Mroz, P., Nowis, D., Piette, J., Wilson, B. C., & Golab, J. (2011). Photodynamic therapy of cancer: An update. *CA Cancer J Clin*, 61(4), 250-281. doi: 10.3322/caac.20114.